Clim Dyn (2015) 44:1505–1519
DOI 10.1007/s00382-014-2180-y

Impact of intraseasonal oscillation on the tropical cyclone track in the South China Sea

Lei Yang · Yan Du · Dongxiao Wang · Chunzai Wang · Xin Wang

Received: 24 October 2013 / Accepted: 13 May 2014 / Published online: 28 May 2014

Abstract This study investigates the impact of the intraseasonal oscillation (ISO) on tropical cyclone (TC) tracks in the South China Sea (SCS) during 1970–2010. About one third of TCs in the SCS move eastward, while the other two thirds move westward. In the TC genesis peak seasons of June–October (JJASO), the westward moving TCs are controlled by the background TC steering flow of easterly, and the eastward moving TCs by the TC steering flow induced by the ISO. The outgoing longwave radiation and wind fields show that the eastward moving TCs were mostly along the main axis of strong TC steering flow anomaly of westerly associated with the ISO, while the westward moving TCs were only weakly associated with the ISO. An experiment performed with a simple two-level model further confirmed the result. The interannual variation of TC tracks in the SCS is also discussed. It is found that the steering flow anomalies in the SCS mostly favor eastward moving TCs in central Pacific (CP) El Niño and eastern Pacific (EP) El Niño years. However, the eastward flow anomalies are too weak to have strong influence on the majority of the TCs. During La Niña years, TCs in the SCS tend to move westward, possibly related to the westward steering flow anomalies.

Keywords The South China Sea · Tropical cyclone · Track · Steering flow · Intraseasonal oscillation · ENSO

L. Yang · Y. Du (✉) · D. Wang · X. Wang
State Key Laboratory of Tropical Oceanography (LTO), South China Sea Institute of Oceanology, Chinese Academy of Sciences, 164 West Xingang Road, Guangzhou 510301, China
e-mail: duyan@scsio.ac.cn

C. Wang
NOAA/Atlantic Oceanographic and Meteorological Laboratory, Miami, FL, USA

1 Introduction

Tropical cyclones (TCs) induce serious losses of life and property damages over coastal areas via strong winds, torrential rainfall, and tidal surges during or after making landfall (Chan et al. 2004; Gemmera et al. 2011). The prediction of landfall location is therefore of economic, social, and scientific significance (Liu and Chan 2003). TC geneses location, frequency and intensity, and track direction are the main factors determining the TC landfall activities (Wu et al. 2004; Goh and Chan 2010).

Tropical cyclone genesis is closely related to dynamic and thermodynamic factors such as sea surface temperature (SST), midtroposphere moisture, and vertical wind shear (Gray 1979; Camargo et al. 2007a; Chia and Ropelewski 2002). The variations of TC genesis frequency and intensity in the western North Pacific (WNP), from seasonal to interdecadal time scales, have been related to monsoon trough (e.g., Xie et al. 2003; Wang et al. 2007; Wu et al. 2012), El Niño-Southern Oscillation (ENSO) (e.g., Chan, 1985, 1995; Chan and Xu 2009; Chen 2011; Du et al. 2011; Zhan et al. 2011), and Pacific Decadal Oscillation (PDO) (Goh and Chan 2009; Liu and Chan 2008, 2013). The variation of TC geneses was also found closely related to the intraseasonal oscillation (ISO) over the WNP (Gray 1979; Nakazawa 1988; Liebmann et al. 1994; Sui and Lau 1992; Ko and Hsu 2009; Camargo et al. 2009; Sobel and Maloney 2000; Huang et al. 2011, hereafter referred to as "H11"; Li et al. 2012; Li and Zhou 2013a). Around 70 % of TCs in the WNP formed during the active ISO period of June to December (H11). TC geneses tend to cluster near the cyclonic circulation during ISO active phase, with an enhanced monsoon trough and a moisture confluent zone, while TC geneses are infrequent and poorly organized in the ISO

inactive phases due to unfavorable large scale environmental conditions (Ko and Hsu 2009).

Other than TC geneses, TC track direction is the main factor related to TC landfall activities (Liu and Chan 2003). Understanding the mechanisms influencing TC track direction is of great importance to the prediction of TC landfall. TC track direction is mainly determined by two processes: advection of the relative vorticity by large-scale environmental flow and beta drift (Wang et al. 1997). TC tracks in WNP have been classified into different types using different cluster methods and related with large scale circulation (e.g., Camargo et al. 2007b, 2007c; Kim et al. 2010). Large-scale environmental steering flow is the dominating external influence on a TC, accounting for 70–90 % of a TC movement (Neumann 1992). Numerical and observational studies suggest that the beta drift term becomes important in causing a systematic deviation only when the TC steering flow is relatively weak (Carr and Elsberry 1990; Wang and Li 1992; Franklin et al.1996; Wang and Holland 1996). TCs that do not follow the environmental background steering flow should be guided by anomalous steering flow induced by other factors (Emanuel 1991; Chan 1995; Wu and Emanuel 1995).

ENSO is a powerful interplay between the tropical ocean and atmosphere in the Pacific basin. Large scale circulation anomalies associated with ENSO is thus the important factor influencing the TC track direction on interannual time scale. TC tracks in the WNP and the landfalls in East Asia related El Niño and La Niña have been investigated in numerous studies (e.g., Saunders et al. 2000; Sobel and Maloney 2000; Wang and Chan 2002; Liu and Chan 2003; Wu et al. 2004; Camargo and Sobel 2005; Fudeyasu et al. 2006; Lyon and Camargo 2009; Zhang et al. 2012). Previous studies have identified the important impact of ENSO on TC genesis location over the WNP, with a displacement of the mean TC genesis region to the southeast (northwest) during El Niño (La Niña) years, respectively (e.g., Wang and Chan 2002; Chia and Ropelewski 2002; Yonekura and Hall 2011). The displacement of TC genesis location can lead to different track characteristics. There is an enhanced tendency of the cyclones in El Niño years to recurve northeastward and reach more northward latitudes (Wang and Chan 2002; Elsner and Liu 2003; Zhang et al. 2013). Different types of TC track was found closely related to the anomalous large-scale winds associated with different ENSO phases (Wu and Wang 2004). The differences in TCs making landfall over East Asia between El Niño and La Niña are detected only during autumn (Wang and Chan 2002; Wu et al. 2004). The conventional El Niño, also called Eastern Pacific (EP) El Niño, involves temperature anomalies in the EP. However, in the last two decades, a new type of Pacific warming was observed in the central Pacific Ocean, referred as El Niño Modoki (Ashok et al. 2007), or central Pacific El Niño (CP El Niño, Kug et al. 2009). The mechanisms of different ENSO events on TC track variabilities in the WNP have been widely studied (e.g. Chen and Tam 2010; Hong et al. 2011; Kim et al. 2011; Wang and Wang 2013). During CP El Niño years, TCs tend to recurve northward at a further westward location and make landfall to Taiwan and southern China due to the westward shift of subtropical High and associated steering flow (Hong et al. 2011). They suggest the warming SST in the WNP as the cause. Zhang et al. (2012) demonstrate that WNP TCs have a remarkable tendency to make landfall over East Asia (Korea and Japan) during the summer of CP El Niño years because of a strong easterly steering flow anomaly, which lead to westward moving TCs. They also found that more (less) TCs are likely to make landfall in China, Indochina, the Malay Peninsula, and the Philippines during the peak TC season of La Niña (EP El Niño) years.

Several studies have identified the impact of ISO on the TC track and landfall activity in the WNP. For example, Kim et al. (2008) found that a dense area of tracks migrates eastward (westward) when the ISO convection is located near the equatorial Indian Ocean (IO) (tropical WNP). Chen et al. (2009) related the intraseasonal variation of TC tracks with that of the monsoon trough and the subtropical high. They demonstrated that the straight-moving TCs are linked to an intensified subtropical anticyclone, while the recurving TCs are usually associated with a deepened monsoon trough. TC tracks in the WNP is found to be closely related to low level ISO wind fields, especially vorticity (Tian and Li 2010; Tian et al. 2010). Li and Zhou (2013b) found that during the active phases of ISO, westward and northwestward moving TCs dominates in the WNP because of the strong easterlies (southeasterlies) in the southern flank of the subtropical high, while during the inactive phase of ISO, TCs in the WNP switch to recurving type, leading to more TC activities at the southeast of Japan.

The South China Sea (SCS), a large semi-enclosed marginal sea in the WNP, is an active basin of TC genesis, accounting for 13 % of the total TCs in the WNP (Wang and Fei 1987). This study finds that the tracks of TCs that generated in the SCS can be divided into two categories: westward (including straight westward, northwestward and southwestward), and eastward (including straight eastward, northeastward, and southeastward) movements. TCs moving eastward easily made landfall at the Philippines, Taiwan, Japan, or occasionally recurved back to reach the southern China coast (Fig. 1a), while those westward moving TCs tended to make landfalls on the southern China and Vietnam coast (Fig. 1b). Previous studies mainly focus on the variations of westward, northwestward and recurving TCs in the WNP (e.g., H11; Kim et al. 2011;

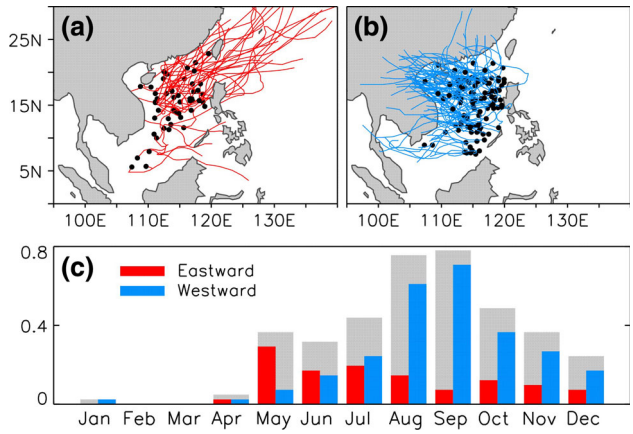

Fig. 1 TC tracks over the period of 1970–2010: **a** eastward TC during April–December (landfall location is at the east of TC genesis); **b** westward TC (landfall location is at the west of TC genesis) during April–December; **c** seasonal cycle of numbers of eastward (*red*), westward (*blue*) and total TCs (*gray*). *Black dots* in **a** and **b** mark TC genesis location

Zhang et al. 2012; Li and Zhou 2013b). Although the TCs that form in the SCS are more or less included in the previous studies, the unique track directions and influences from local forcings are not fully considered. The purpose of this study is to fully examine the mechanisms of the westward and eastward TC tracks in the SCS, and reveal the relationship between TC tracks and large scale circulation anomalies.

The paper is organized as follows. Section 2 introduces the datasets and methods employed in the study. Section 3 reveals the seasonal variation of TC track directions in the SCS. Section 4 investigate the relationships of the ISO with westward and eastward TC tracks during different periods, followed by the discussions of the possible mechanism for the impact of ISO on TC tracks and the interannual variations of TC track directions in Sect. 5. The relationship of TC track directions and ENSO events (including CP El Niño, EP El Niño and La Niña) are also discussed in Sect. 5. Finally, a summary is given in Sect. 6.

2 Data sets and method

2.1 Data sets

The best-track dataset from the Joint Typhoon Warning Center (JTWC) is used in this study. It includes TC location and intensity at 6-h interval and covers the IO, the SCS and the WNP. A TC is defined as a storm with enclosed cyclonic circulation and sustained winds of 25kts or above. This study focuses on the SCS and the 41-year period of 1970–2010.

Convection associated with the ISO is based on the interpolated outgoing longwave radiation (OLR) from the National Oceanic and Atmospheric Administration (NOAA), which is daily data on a 2.5° × 2.5° grid from 1979 to 2010 (Liebmann and Smith 1996).

Horizontal wind data at standard vertical are derived from the US National Centers for Environmental Prediction (NCEP) reanalysis with a horizontal resolution of 2.5° latitude × 2.5° longitude (Kalnay et al. 1996). An integrated flow through a layer of atmosphere is usually defined as steering flow (Dong and Neumann, 1986), which is commonly used to represent the mean-state of the large scale circulation to the overall TC motion (e.g., Holland 1983). The choices of atmosphere layer are diverse in different studies. For example, a layer from 850 to 300 hPa is used to compute steering flow in Chu et al. (2012), while the average wind through a layer from 900 to 200 hPa was considered best correlated with TC movement in Chan and Gray (1982). Ideally, the steering flow of a TC should be calculated as an area-average vertically integrated wind around the storm (Chan and Gray 1982). To simplify the analysis, vertically integrated wind at grid points of reanalysis data is computed, without following a storm (Chu et al. 2012). In this study, we compute the steering flow by vertically integrate the pressure-weight flow from the 850 to 200 hPa. The results are similar if we choose 300 hPa (900 hPa) instead of 200 hPa (850 hPa) in the calculation.

A 20–100 day bandpass filter is performed on daily data (hereafter as "filtered" data vs. original data). To analyze the interannual variability associated with ENSO activities, the Niño3.4 index is calculated using the SST anomaly averaged over the Niño 3.4 region (5°S–5°N, 120°–170°W).

In order to compare the impacts of different ENSO events on the TC tracks, El Niño Modoki index (EMI) and the Niño-3 index are utilized. Niño-3.4 index is usually used to determine El Niño and La Niña; however, it fails to distinguish two types of Pacific warming events (Chen and Tam 2010). The monthly indexes are directly downloaded from the National Oceanic and Atmospheric Administration (NOAA) Climate Prediction Center. The EMI is used to measure the SST anomaly in the central Pacific (Ashok et al. 2007), which is defined as

$$\mathrm{EMI} = [\mathrm{SSTA}]_{\mathrm{A}} - 0.5[\mathrm{SSTA}]_{\mathrm{B}} - 0.5[\mathrm{SSTA}]_{\mathrm{C}}$$

where $[\mathrm{SSTA}]_{\mathrm{A}}$, $[\mathrm{SSTA}]_{\mathrm{B}}$, and $[\mathrm{SSTA}]_{\mathrm{C}}$, denote the SST anomaly averaged over the regions, A (10°S–10°N, 165°E–140°W), B (15°S–5°N, 110°–70°W), and C (10°S–20°N, 125°–145°E), respectively. The months during which EMI and Niño-3 index are warmer than one standard deviation and the Niño-3 index is cooler than one standard deviation are defined as the CP El Niño, EP El Niño and La Niña,

respectively, after the linear trends are removed from these time series of indexes (Chen and Tam 2010; Zhang et al. 2012). Thus, 6 CP El Niño years (1977, 1990, 1991, 1994, 2002 and 2004), 6 EP El Niño years (1972, 1976, 1982, 1983, 1987, and 1997), and 6 La Niña years (1970, 1973, 1975, 1988, 1999, and 2007) are defined, in order to further investigated the impact of different type of ENSO events.

2.2 A simple model

The simple model used in this study is developed by Lee et al. (2009). This is a two-level model, in which equations are recast as baroclinic and barotropic components and are linearized about prescribed background wind fields. The model is designed to simulate both the local and remote stationary response of the atmosphere when forced with a localized heating. In this model, the baroclinic response to tropical heating anomalies is essentially the same as described by the Matsuno–Gill model (Matsuno 1966; Gill 1980). This baroclinic response then excites a barotropic response by advective interactions with vertical background wind shear (i.e., through the shear advection mechanism), and the barotropic signals are in turn transmitted to high latitudes.

3 Seasonal variability in the TC tracks

154 TCs formed in the SCS from April to December during 1970–2010, among which 105 TCs moved westward and 49 moved eastward. While the westward TC numbers show pronounced annual cycle with peak in September, eastward moving TCs display less variability with peak in May (Fig. 1c). The 13th TC in 1986 was not included due to its very complicated track. Although the total TC number during May–July is similar, there is significant change in the proportion of eastward to westward TC numbers which peaks in May (great than one), decreases largely in June and reverses to less than one in July (Fig. 1c). The westward TCs outnumber eastward TCs from July to December. The reason for the seasonal variation of the proportion of eastward and westward TCs will be discussed in detail in next section.

The TC geneses mainly distributes in the northern SCS during June–October and shift to the southern SCS after November (Fig. 2). The TC genesis locations are closely related to the monsoon trough (Xie et al. 2003; Wang et al. 2007). The summer monsoon trough becomes active in the SCS after May, lingers in the northern SCS until September and then moves to the southern SCS (Liang 1991). The monthly-mean TC genesis locations tend to lag the north-to-south shift of the monsoon trough by a few degrees of latitude (Chia and Ropelewski 2002). For example, the mean TC geneses locations in October are still in the northern SCS ($\sim$13°N), while the monsoon trough already moves to the southern SCS (south of 10°N) (Wang et al. 2007). Based on the variation of the monsoon trough and mean TC locations, the TC season is further divided into three periods: April–May (AM), June–October (JJASO) and November–December (ND). JJASO is considered as the peak TC season, since most of TC form during the period (Fig. 1c).

The TC tracks and steering flows for AM, JJASO and ND are shown in Fig. 2. During AM, TCs tended to move eastward (71 % of TCs move eastward). The westward-moving TCs during AM formed farther south (south of 13°N) where the TC steering flow is easterly, while those eastward-moving TCs formed in the area where the TC steering flow was in the transition from southeasterly to northwesterly. During JJASO, most of TCs (84) moved westward, while 29 TCs moved eastward. Most TCs formed in the northern SCS during the time when it was mainly controlled by the southeasterly TC steering flow. During ND, 24 TCs formed in the SCS, with 17 moving westward and 7 eastward. The TC steering flow pattern during ND was very similar to that during AM. The combined effects of the track direction and location of TC genesis in the far south during ND could lead to major landfall events on the Vietnam coast and rare landfall activities on the southern China coast, Japan and Taiwan Island.

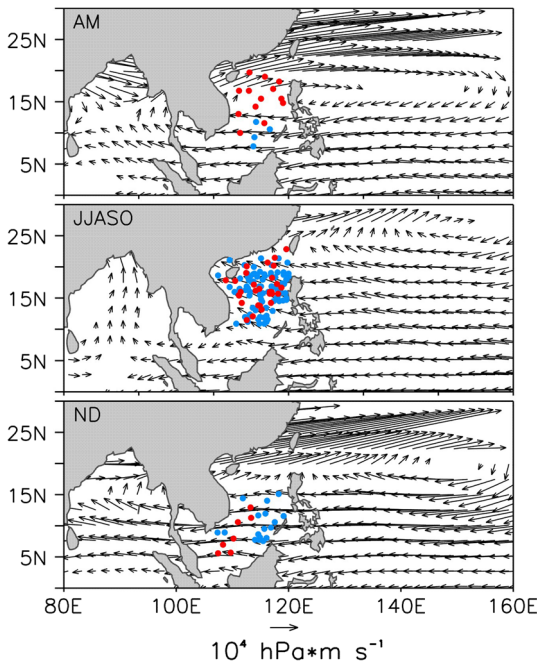

Fig. 2 Background steering flow (average during 1970–2010) for April and May (AM), June to October (JJASO) and November and December (ND). For better illustration, vectors smaller than 0.5x10^4 hPa m s^{-1} are omitted. *Red* (*blue*) dots marks genesis location for eastward (westward) moving TCs

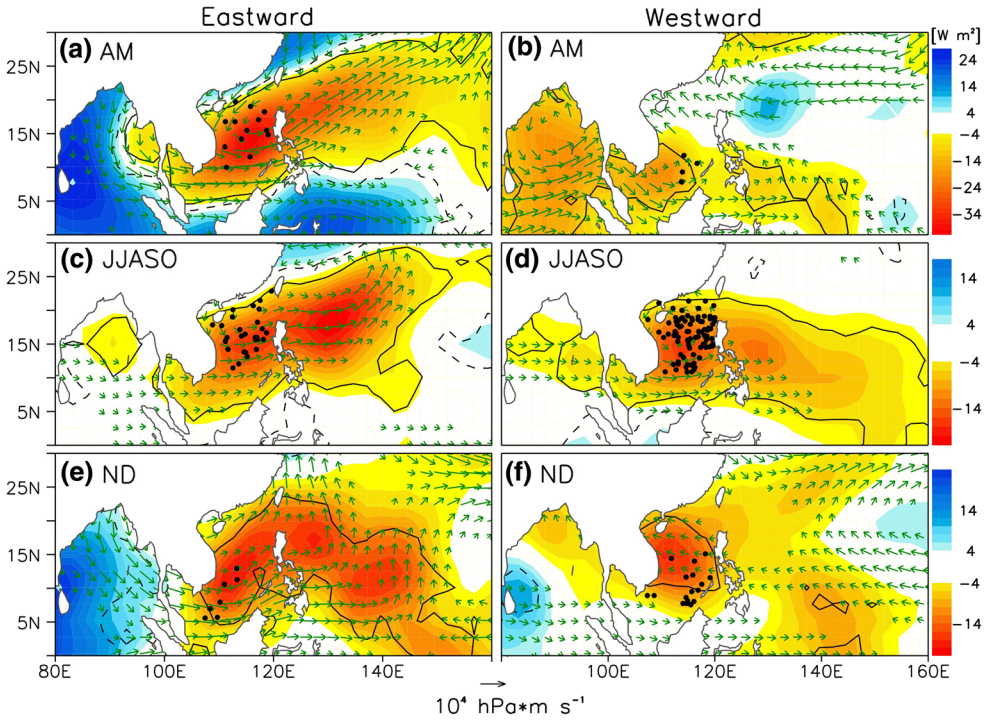

Fig. 3 Composites of 20–100 day filtered steering flow anomaly (*vector*; hPa m s^{-1}) and OLR anomaly (*shaded*; W m^{-2}) for eastward and westward moving tracks during April and May (AM), June to October (JJASO) and November and December (ND). The contour lines (*vectors*) indicate that the differences of the OLR (*steering flow*) anomalies exceeding the 95 % significant level based on a Student's *t* test. For better illustration, vectors smaller than $0.5x10^4$ hPa m s^{-1} are omitted

The TC tracks during AM, both the eastward and westward moving, match very well with the direction of background steering flow. However, it is not the case for the TC tracks during JJASO and ND. During these two periods, a significant portion of TCs moved eastward, against the background TC steering flow. Next, we try to understand what forced these TCs to move eastward.

4 Impact of ISO on the TC tracks

Composites of the 20–100 day bandpass-filtered OLR and corresponding TC steering flow anomaly (3-day average after the TC genesis) for the eastward and westward TC track cases are shown in Fig. 3. OLR is a good proxy for tropical deep convection (e.g., Lau and Chan 1985; Salby and Hendon 1994; Nakazawa 1995; Matthews 2008; Riley et al. 2011). We use filtered OLR as local phase (Riley et al. 2011) to determine ISO activity, in contrast to the global phase of the ISO. The latter is usually defined using a popular real-time multivariate Madden–Julian oscillation (MJO) index (RMM), which assigns the tropics to an MJO phase each day and does not depend on the season (Wheeler and Hendon 2004). The RMM index cannot accurately describe the northward propagation of ISO over the WNP when ISO propagates northward north of 30°N in the boreal summer (H11). Local phase defines the ISO signal based on the filtered OLR value at each longitude and time (Riley et al. 2011). Large negative OLR value represents an active ISO phase (Matthews 2008). The dominant signals of ISO mainly propagate eastward during boreal winter (Madden and Julian 1971). However, in boreal summer, WNP ISO propagates not only eastward but also northward into subtropics (Chen and Murakami 1988). The propagation of ISO has a significant seasonal variation during the WNP TC season (H11), with large difference between the early summer and late summer. In H11, the propagations of ISO from IO to WNP for different periods were classified into eight phases based on EOF analysis of 30–90-day filtered OLR field. The eight phases were then grouped into four phases, phases 1 & 2, 3 & 4, 5 & 6 and 7 & 8 according to the strength of TC geneses activities, among which phases 5 & 6 represents the strongest convection. In early summer, positive convection anomalies in the Maritime Continent (phases 1 & 2, Fig. 4a in H11) propagate along two directions, eastward into far southeast of the Philippine Sea and northward into the SCS (phases 3 & 4, Fig. 4b in H11) and then converge around the Philippine Sea in phases 5 & 6 (Fig. 4c in H11). The negative convection anomalies at marine continent in phases 5 & 6 propagate southeast of the Philippine Sea and the SCS in phase 7 & 8 (Fig. 4d in H11). The two isolated

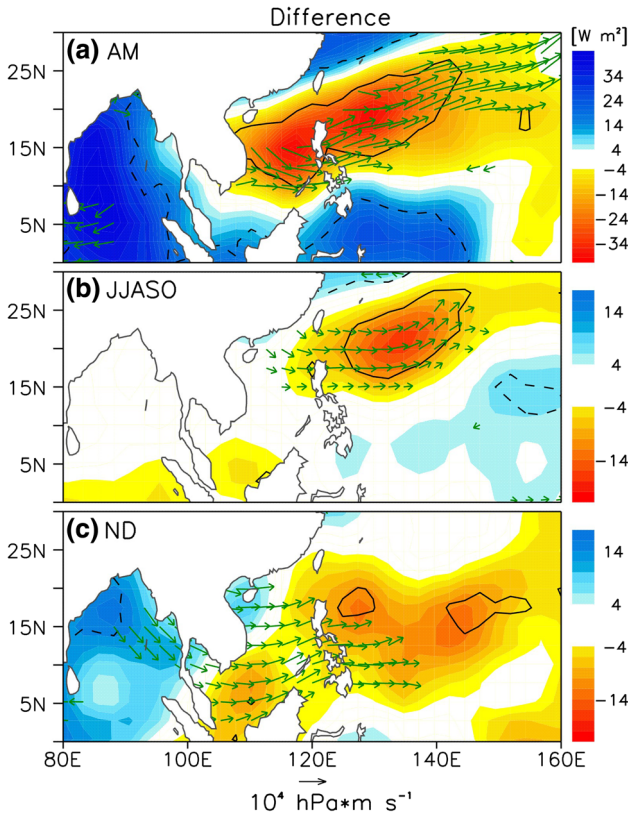

Fig. 4 Differences of 20–100 day filtered steering flow anomaly (*vector*; hPa m s^{-1}) and OLR anomaly (*shaded*; W m^{-2}) between westward and eastward (westward–eastward) moving tracks during April and May (AM), June to October (JJASO) and November and December (ND). The contour lines (*vectors*) indicate that the differences of the OLR (*steering flow*) anomalies exceeding the 95 % significant level based on a Student's *t* test

negative convection anomalies converge around the Philippine Sea in the next phases, 1 & 2. During late summer and early fall, positive convection anomalies develop in tropical western Pacific (phases 1 & 2, Fig. 7a in H11) and move northward to around 10°N (phases 3 & 4, Fig. 7b in H11) via two routes and then gathers at the Philippine Sea (phases 5 & 6, Fig. 7c in H11). The negative convection anomalies over the Maritime Continent during phases 5 & 6 propagate northward into tropical western Pacific (phases 7 & 8, Fig. 7d) and then farther into the Philippine Sea in the next phases 1 & 2.

4.1 AM

Figure 3a, b show that eastward TCs mainly clustered in the northern SCS (north of 10°N), while westward TCs occurred in the central SCS (around 10°N). Both of the areas were under the influence of negative OLR anomaly, indicating positive convection. The positive convection during the eastward TC cases is much stronger and significant, covering whole northern SCS and extending further northeast into WNP (Figs. 3a, 4a). On the contrary, during westward TC case, only weak positive convection appears over the area south to 10°N in the SCS. It is also noticed that the convection in IO for the two cases displays opposite pattern, i.e., negative (positive) during westward (eastward) TC case. The different pattern of the convection anomaly during the two cases reveals that westward and eastward TCs may occur at two different phase of the ISO during its propagation from IO into WNP. Comparing Fig. 3a, b in this study with Fig. 4b, c in H11, it is found that the convection pattern during the eastward (westward) TC case matches well with the anomaly pattern in phases 5 & 6 (phases 3 & 4). The significantly strong westerly steering flow anomalies dominating from the SCS to WNP, induced by the corresponding convection, may contribute to the eastward tracks of TCs that formed in the northern SCS. Weak steering flow anomalies for the westward TC cases obviously have less impact of the TCs in the central SCS. The flow anomaly induced by the ISO activities is comparable to the original flow (Fig. 5a) for eastward TCs, suggesting the important role of the ISO on TC movement.

4.2 JJASO

During JJASO, large positive convection dominated the entire SCS and part of the WNP in both westward and eastward TC cases. For the eastward moving TCs, the positive convection anomaly oriented from southwest to northeast with two maxima, located at the west (in the northern SCS) and east of the Philippines, respectively. The convection center east of Philippines is even stronger than that in the northern SCS. The ISO-induced TC steering flow anomaly was strong over the area where most eastward moving TCs formed and extended to the WNP with stronger magnitude (Figs. 3c, 4b). It is found that most of the eastward TCs are distributed along the main axis of the eastward flow, indicating the importance of the anomalous steering flow (Fig. 3c). The magnitude of ISO-induced TC steering flow anomaly over the area for the eastward TC case was comparable to that of the original TC steering flow (Fig. 5c).

For the westward moving case, the WNP including the SCS was also dominated by positive convection (Fig. 3d). However, both the convection strength and its induced TC steering flow anomaly in the SCS and WNP were much weaker, comparing to those during the eastward moving case. The positive convection anomaly oriented from west to east. The TC steering flow anomaly over the area where most TCs occurred was much smaller than original steering flow, imposing a smaller effect on the TC movement compared to the background steering flow (Fig. 5d). Relatively large TC steering flow anomaly can be seen in the

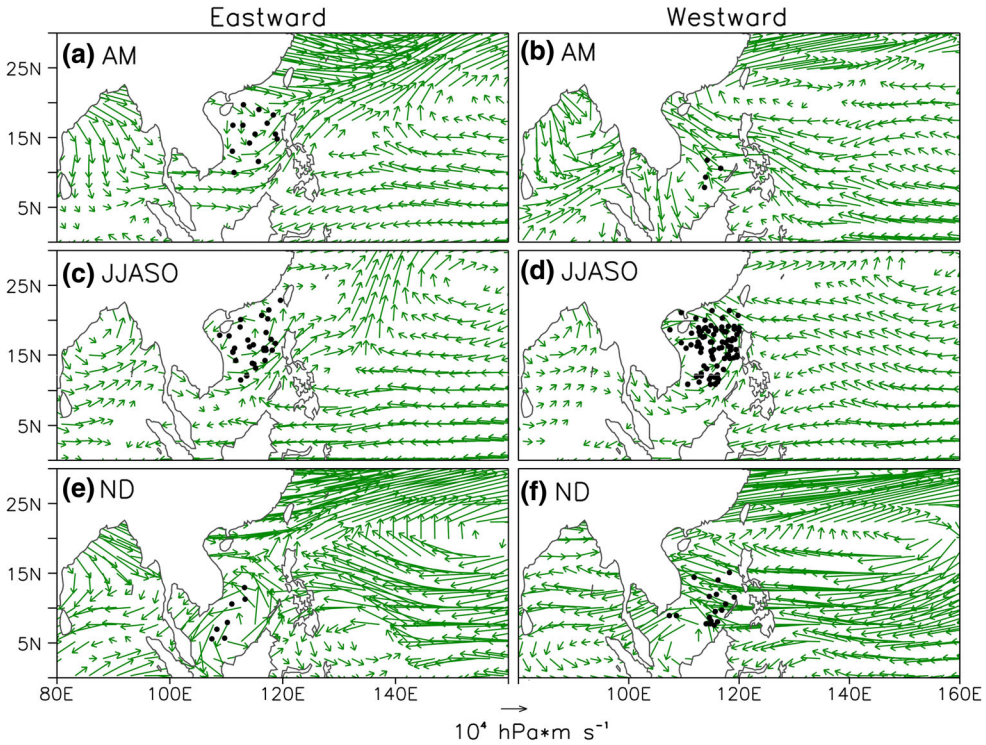

Fig. 5 Composites of original steering flow (*vector*; hPa m s^{-1}) for eastward and westward moving tracks during April and May (AM), June to October (JJASO) and November and December (ND). For better illustration, vectors smaller than $0.5x10^4$ hPa m s^{-1} are omitted

southern SCS where usually no TC forms during JJASO (Xie et al. 2003; Wang et al. 2007).

During late summer, the ISO propagated from the IO into the low-latitude western Pacific, and then almost synchronously propagated northward through the SCS and the WNP routes (Wang and Rui 1990; H11). The favorable conditions for the TC geneses moved northward into the SCS and WNP, accompanied by the propagation of the ISO. Comparing Fig. 3c, d with Fig. 7b, c, in H11, it is found that the strong convection in the SCS and WNP with much stronger convection located in the WNP (overall weaker and more relax convection pattern) during eastward (westward) TC case matches well with those of phases 5 & 6 (phases 3 & 4) in H11. It indicates that only peak active phase of ISO can induce strong westerly anomalies that can overpower the background easterly (Fig. 4b).

To further examine the seasonal variation of the TC tracks and their relations with ISO, the peak TC season of JJASO is subdivided into two parts: JJA and SO. It is found that most of the eastward moving TCs during JJASO formed during JJA (72 %), while the westward moving TCs have similar amount during JJA (40) and SO (44) (Fig. 6; Table 1). ISO related convection anomaly pattern is similar between JJA and SO for both eastward and westward moving TC cases. For eastward cases, there are two convection centers (the SCS and WNP) in both JJA and SO, with relatively stronger convection anomalies in the SCS (WNP) during SO (JJA). Moreover, the anomaly patterns are obviously more compact during JJA comparing to that during SO. During JJA, ISO related convection extends from the SCS to northwestern WNP with a maximum centered at the west ocean area of Luzon strait, inducing significantly enhanced easterly flow (Figs. 6a, 7a). However, the convection pattern split into two parts during SO, one located at the SCS, presenting a west-east pattern, the other one at the west of the Philippine Islands with the southwest-northeast orientation (Fig. 6c). The overall effects of the changes in the convection pattern form JJA to SO is that the steering flow anomalies induced by the two convection centers during SO counteract each other, leading to rather small westerly flow anomalies in the SCS and WNP. The westerly flow anomalies at the east of Philippines are significant larger than that in the SCS (Fig. 7b). The flow anomalies for westward TCs are much smaller comparing to eastward TC cases, especially for those during SO (Fig. 6b, d). It is obvious that ISO related steering flow anomalies during JJA contribute the most of the eastward TCs during JJASO (Fig. 7). While the ISO-induced westerly steering flow anomalies during eastward TC cases are comparable to that of the original TC steering flow, small steering flow anomalies during westward TC cases can not overpower the strong easterly background steering flow, therefore has weak effects on westward TC tracks (Fig. 8).

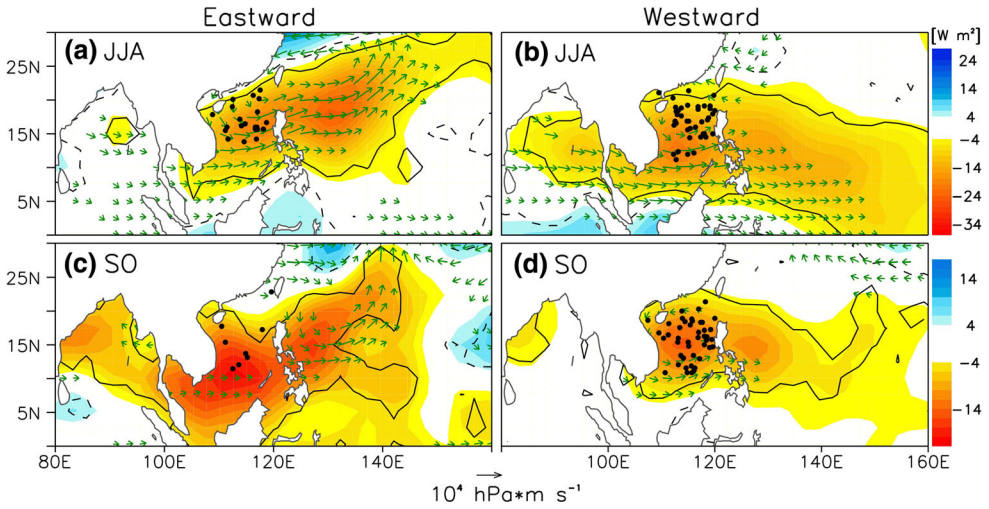

Fig. 6 Composites of 20–100 day filtered steering flow anomaly (*vector*; hPa m s^{-1}) and OLR anomaly (*shaded*; W m^{-2}) for eastward and westward moving tracks during June–August (JJA) and September–October (SO). The contour lines (*vectors*) indicate that the differences of the OLR (*steering flow*) anomalies exceeding the 95 % significant level based on a Student's *t* test. For better illustration, vectors smaller than $0.5x10^4$ hPa m s^{-1} are also omitted

Large scale circulation also displays strong differences for eastward and westward cases during JJA and SO. Figure 9 shows the 850 hPa wind anomalies and western North Pacific High (WNPSH, denoted by 5870 geopotential height) for the two cases during JJA and SO. For the eastward TC cases, anomalous strong southwesterly wind anomalies dominate the SCS and northwest of the Philippines during JJA. In the meantime, WNPSH retreated to 135°E, about 20 degree east to the climatological location (Fig. 9a). The anomalous low level westerly flow decreased greatly during SO, especially over the SCS (Fig. 9c). WNPSH during SO locates at approximately similar longitude to that during JJA. This type of large scale circulation can also lead to relatively more recurving TCs in the WNP, causing more landfalls over Japan (Li and Zhou 2013b). For the westward TC case, the WNP (including the SCS) is controlled by an east–west orientated, low-level cyclonic circulation, with westerly (easterly) in the southern (northern) SCS (Fig. 9b). The strength of the circulation is much weaker comparing to that of eastward cases. For the westward case, the location of WNPSH is similar to the climatology, with northward shift comparing to the eastward case. The low level circulation for the westward case during SO is very similar to that during JJA, with smaller magnitude and more westward extension of WNPSH (Fig. 9d). As clearer shown in Fig. 10, the pattern of WNPSH during eastward TC cases favors westerly flow at the west edge of WNPSH, steering the TCs in the SCS to eastward, while the northwest extension of WNPSH lead to northeasterly or easterly at the northern SCS and WNP.

4.3 ND

The TC genesis location shifted to the southern SCS during winter season (Fig. 3e, f; Xie et al. 2003; Wang et al. 2007). For the eastward TC case, positive convection and significant northeastward TC steering flow anomaly shifted farther south, corresponding well with the TC locations (Figs. 3e, 4c). Convection and TC steering flow anomaly for the westward moving TC case were weaker than those during eastward TC case, indicating a weaker influence from ISO variation (Fig. 3f). Strong anticyclonic circulation appears in original steering flow during ND for both eastward and westward TC cases (Fig. 5e, f). The outflow at the west edge of the anticylonic system direct westward into the SCS for westward TC cases. However, during eastward TC cases, the flow directs northeastward around 140°E and therefore have less impact on the TC tracks in the SCS, especially the Southern SCS. The change of the flow direction is very likely related to the strong ISO activities, which induces significant westerly in the southern SCS, leading TCs in the area moving eastward (Fig. 4c).

To further confirm the relationship between convection activity and its induced steering anomalies, two OLR anomalies for eastward and westward cases during JJASO are added in a simple two-level model of Lee et al. (2009). During eastward case, we can see a cyclonic circulation over the East Asia and large anticyclonic circulation over the WNP, orienting southwest to northeast and extending to 30°N (Fig. 11a). Correspondingly, strong westerly (the sum of the two levels—750 hPa and 250 hPa) forced with OLR anomaly during eastward TC case flows through the

Table 1 The statistics of TC numbers in the SCS for AM, JJASO, ND

Season	Eastward	Westward	Total
AM	13	4	17
JJASO	29	84	113
JJA	21	40	61
SO	8	44	52
ND	7	17	24
Total	49	105	154

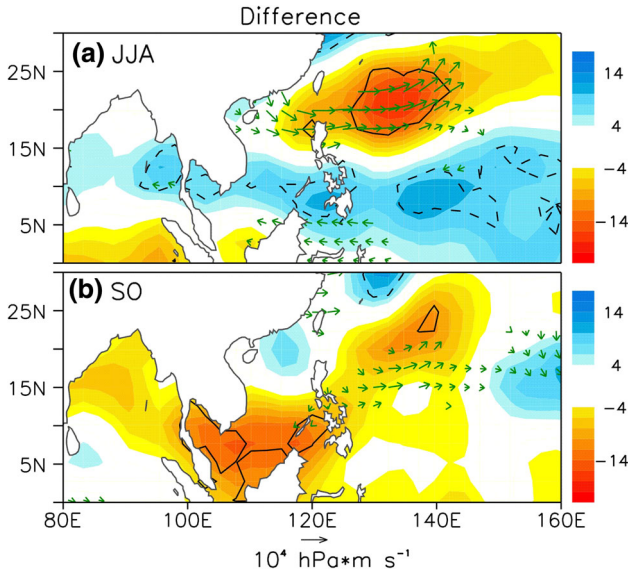

Fig. 7 Differences of 20–100 day filtered steering flow anomaly (*vector*; hPa m s^{-1}) and OLR anomaly (*shaded*; W m^{-2}) between westward and eastward (westward–eastward) moving tracks during June–August (JJA) and September–October (SO). The contour lines (*vectors*) indicate that the differences of the OLR (*steering flow*) anomalies exceeding the 95 % significant level based on a Student's *t* test

SCS and northeast to the northern WNP, consistent with that in Fig. 3b. Similar to Fig. 3c, much weaker cyclonic circulation, orientating straight west to east, can be seen during westward TC cases. The westerlies during westward TC case are also much weaker and more relaxed over the SCS (Fig. 11b). The difference between the two cases obviously shows intensified westerlies over the SCS, which should be responsible for the occurrence of the eastward moving TCs (Figs. 4b, 11c).

5 Discussions

5.1 The mechanisms of the impact of ISO on TC tracks in the SCS

Based on the analyses in the Sect. 4, it is found that eastward moving TCs can only appear during peak active phase of ISO, which induces strong westerly anomalies that can overpower the background easterly steering flow. On the other hand, the westward moving TCs mainly occur during sub-active phase of ISO. The weak westerly anomalies associated with sub-active ISO cannot overpower the background easterly. This mechanism can also be used to explain the seasonal cycle of eastward and westward moving TC as described in Sect. 3. In early summer, the background condition is not very mature to TC genesis. Thus, the TC genesis strongly depends on the peak active phase of ISO (H11). In this case, a large part of TCs propagate eastward following the strong steering flow induced by ISO. Conversely, in the late summer and early fall, the environment condition is favorable for TC genesis. Thus, TC can be triggered by sub-active ISO. However, the weak westerly anomalies associated with sub-active ISO cannot overpower the strong easterly background flow.

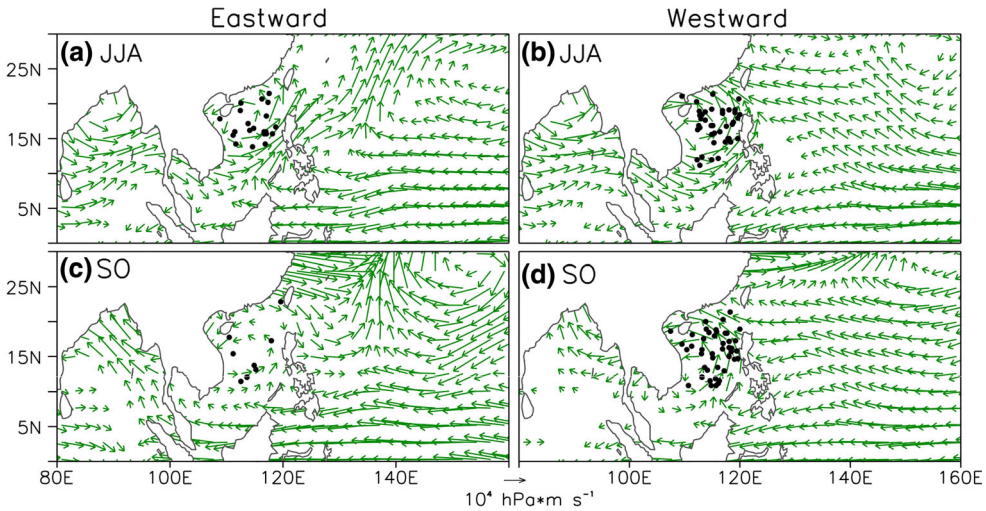

Fig. 8 Composites of original steering flow anomaly (*vector*; hPa m s^{-1}) for eastward and westward moving tracks during June–August (JJA) and September–October (SO). For better illustration, vectors smaller than $0.5x10^4$ hPa m s^{-1} are omitted

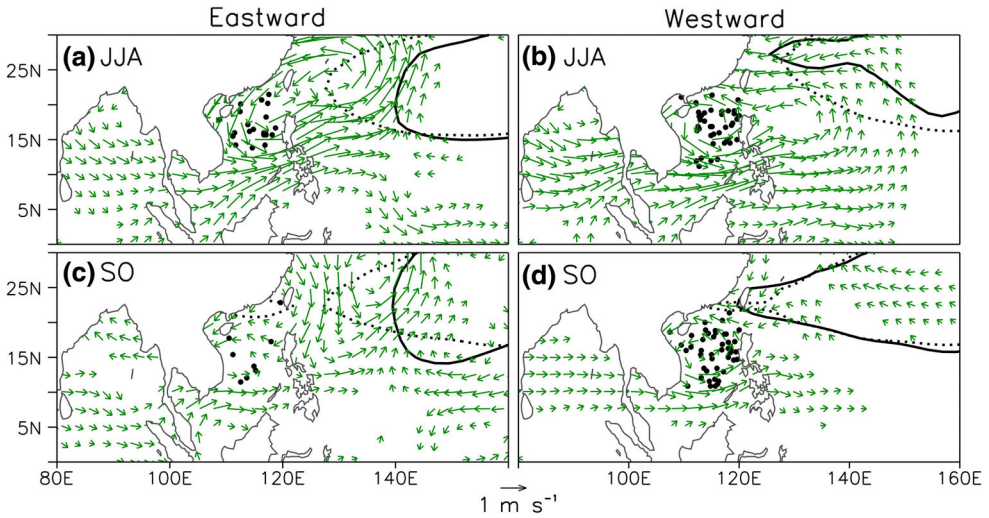

Fig. 9 Composites of 20–100 day filtered 850 hPa anomaly (*vector*; m s^{-1}) for eastward and westward moving tracks during June–August (JJA) and September–October (SO). *Solid contours* denote the 5870 geopotential height, while *dashed contours* denote the climatological 5870 geopotential height. For better illustration, vectors smaller than 0.5 m s^{-1} are omitted

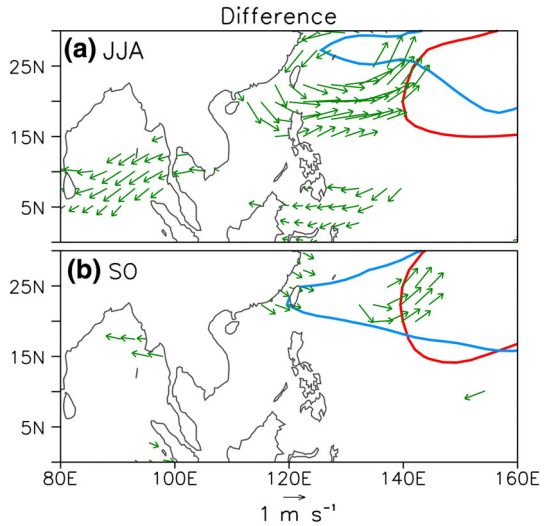

Fig. 10 Difference of the composite of 20–100 day filtered 850 hPa (*vector*; m s^{-1}) between westward and eastward (westward–eastward) moving tracks during June–August (JJA) and September–October (SO). *Solid red* (*blue*) contours denote the 5870 geopotential height for eastward (westward) moving track cases. Vectors indicate that the differences of 850 hPa wind anomalies exceeding the 90 % significant level based on a Student's *t* test

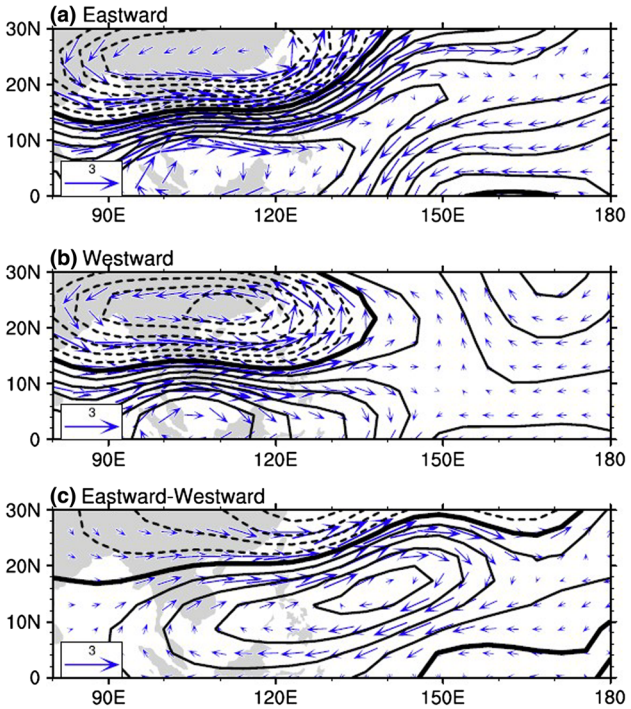

Fig. 11 Barotropic streamfunction (*contour*, 10^6 m^2 s^{-1}) and wind (*vector*, m s^{-1}) from the simple model runs. **a** and **b** are the model responses to the composited OLR anomalies in Fig. 3c, d, respectively. **c** is the differences between **a** and **b** (a − b). The zero lines are *thickened*. The contour interval is 0.5 × 10^6 m^2 s^{-1}

Therefore, there are relatively more eastward moving TCs in May and the proportion of eastward to westward moving TCs decreases greatly in June and reverses to less than one since July (Fig. 1c).

5.2 Interannual variabilities of TC tracks in the SCS

The numbers of westward and eastward moving TCs exhibited strong interannual and longer time-scale variability (Fig. 12). Obviously, the variability was related to the TC genesis frequency, which was mainly controlled by environmental factors (Liu and Chan 2003; Goh and Chan 2009; Chen 2011; Du et al. 2011; Yang et al. 2012). It was found that intraseasonal activities were responsible

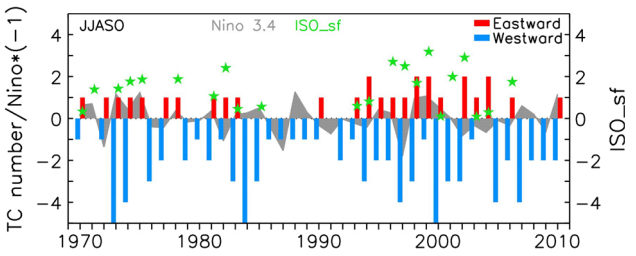

Fig. 12 Interannual variation of TC numbers in the SCS for June to October (JJASO) during 1970–2010, superimposed by the Niño 3.4 index (*gray shading*), zonal component of ISO-induced steering flow during eastward moving TC cases in the area (10°–20°N, 105°–120°E; *green stars* ISO_sf). *Left axis* TC number (negative denotes westward moving) and the Niño 3.4 index (*positive* La Niña event, *negative* El Niño event); *right axis* ISO_sf (*positive* westerly, *negative* easterly)

for the occurrence of the most of eastward moving TCs (Sect. 4). For the eastward TC case during JJASO, the zonal component of ISO-induced TC steering flow anomaly in the TC genesis area (10°–20°N, 105°–120°E) was overall positive, in favor of eastward moving TCs (Fig. 12). It is worth mentioning that there was no direct connection between the TC genesis number and westerly TC steering flow anomaly. In other words, a strong steering flow anomaly of westerly does not lead to more eastward TCs. For example, there were three eastward moving TCs during 1998 and the mean areal (105°E–120°E, 10°N–17°N, same area are referred hereafter for the mean areal average) average of the ISO-induced steering flow anomaly was 1.69 hPa m s^{-1}; while there was only one eastward TC during 2002, but its mean areal average of steering anomaly was 3.6 hPa m s^{-1}, the strongest throughout the 1970–2010 period.

ENSO events can affect TC activity in the WNP (including the SCS), such as the TC frequency, genesis, and intensity (Chan 1985, 2000; Wu and Lau 1992; Wang and Chan 2002; Liu and Chan 2003; Du et al. 2009, 2011). As shown in Fig. 12, the total TC number increased significantly during El Niño decay years, which is consistent with earlier studies (e.g., Du et al. 2011). During El Niño decay years, the warming in the IO excited a warm tropospheric Kelvin wave that propagated eastward, reducing the vertical wind shear over the SCS and leading to more TC geneses (Xie et al. 2009; Du et al. 2011). Li et al. (2012) revealed a stronger modulation of TC genesis by the MJO during El Niño years, while the modulations in neutral and La Niña years were comparable to each other. However, it is still unknown whether the moving directions of TCs formed in the SCS are related to the ENSO events. In this section, the influences of CP El Niño, EP El Niño and La Niña on TC tracks for JJASO and ND periods are discussed. As noted in Zhang et al. (2012), TCs are more

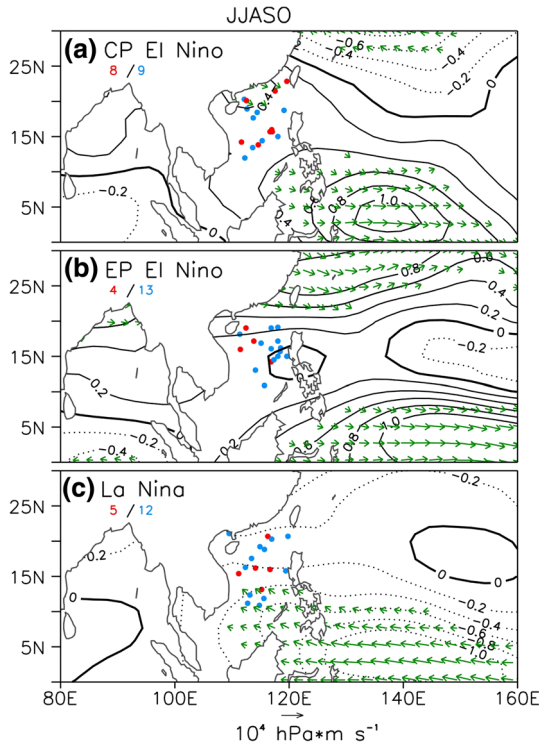

Fig. 13 Composite of steering flow anomalies for CP El Niño, EP El Niño, and La Niña during June–October (JJASO), superimposed by the meridional component of the steering flow anomaly (contour). *Red* (*blue*) numbers in the left corner of each figure represent eastward (westward) TC counts. For better illustration, vectors smaller than 0.5×10^4 hPa m s^{-1} are omitted. *Red* (*blue*) dots represent the genesis location of eastward (westward) moving TCs

likely to make landfall over East Asia during summer (JJA) of CP El Niño, but tend to make landfall over Japan and Korea during the whole peak TC season of JJASO. Therefore, it is necessary to further subdivide JJASO into JJA and SO in the discussions.

5.2.1 JJASO

The composite steering flow anomaly and its meridional component in CP El Niño, EP El Niño, and La Niña Years are shown in Fig. 13. In CP El Niño years, the amount of eastward and westward moving TCs in the SCS is equivalent and the SCS is prevailed by weak westerly (<0.5 hPa m s^{-1}). Stronger westerly and easterly are found at the southern WNP (south to 10°N) and the northern WNP (north to 20°N), respectively. The easterlies at the north were considered as the main factor leading more landfalls of WNP TCs to the East Asian coast during the CP El Niño years (Zhang et al. 2012).

More westward moving TCs are found in the SCS in EP El Niño years. However, the SCS and most of the WNP are mainly controlled by weak eastward steering flow

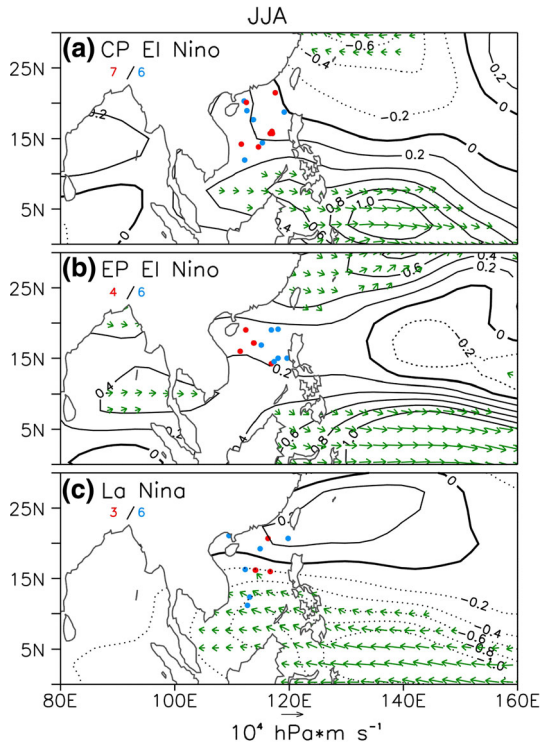

Fig. 14 Same as Fig. 13 but for JJA

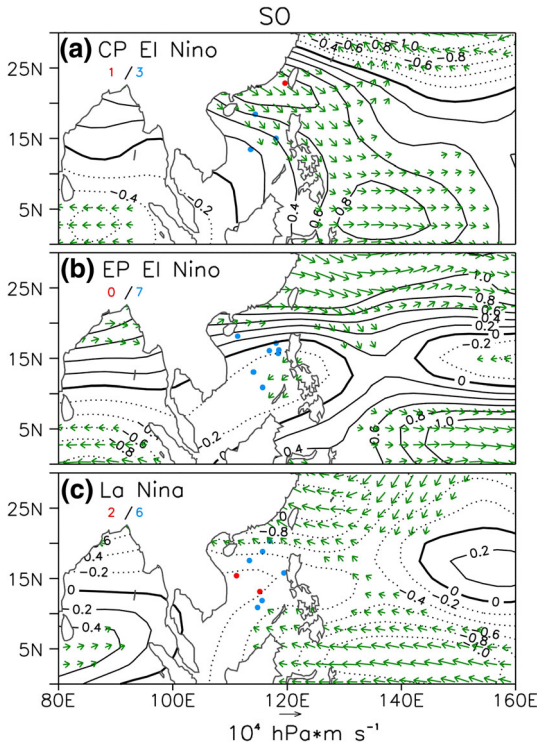

Fig. 15 Same as Fig. 13 but for SO

anomalies, which are in favor of eastward moving TCs. For the WNP TCs, this type of large scale circulation tend to cause TC recurvature over the ocean and to inhibit TC landfall in East Asia (Wang and Chan 2002).

In La Niña years, westward moving TCs (12 out of 17) dominate in the SCS, matching well with the westward steering flow anomalies in the SCS (also most of WNP). Overall westward steering flow anomalies in the WNP favors eastward moving TC tracks and lead to major landfall over China, Indochina, the Malay Peninsula, and the Philippines, and less landfall over Korea and Japan (Zhang et al. 2012).

The proportion of eastward and westward moving TCs, and the pattern (strength)s of steering flow anomalies during JJA are very similar to that of JJASO (Figs. 13, 14). The main difference is that the easterly at the northern WNP is weaker in JJA than that of JJASO, indicating possibly more recurvature of WNP TCs in this area during JJA.

The percentage of westward moving TCs increased in CP El Niño (75 %), EP El Niño (100 %) and La Niña (75 %) years during SO (Fig. 15). In CP El Niño years, the SCS and most of WNP are dominated by much stronger westerlies, compared to that during JJA. In EP El Niño years, westerlies dominate the entire WNP, except the southern SCS, where weak easterlies prevailed. Most of the westward moving TCs are located at the southern SCS, indicating possible steering effect of the easterlies over the

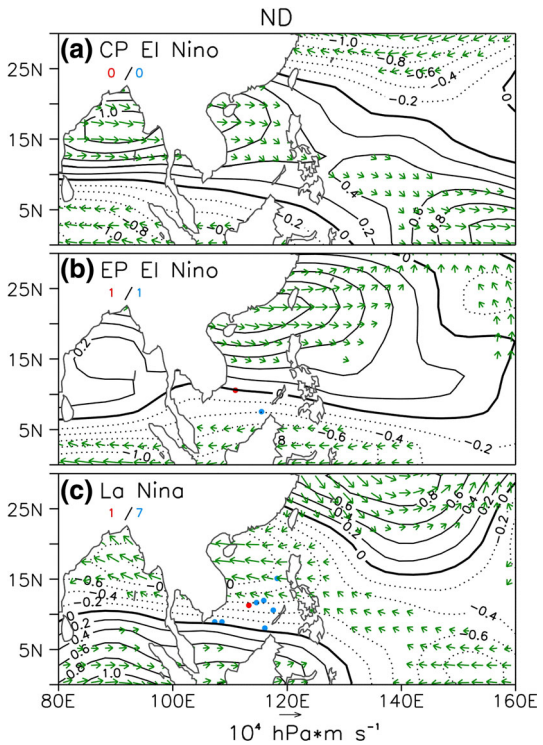

Fig. 16 Same as Fig. 13 but for ND

area. In La Niña years, easterlies are stronger over the northern and southern WNP, but a little weaker in the SCS than that during JJA and JJASO.

5.2.2 ND

During winter, very few TCs occur in CP El Niño and EP El Niño years (Fig. 16). In La Niña years, there are more westward moving TCs (7 out of 9) in the SCS, corresponding well with the strong westward steering flow anomalies in the SCS, especially over the southern SCS, where most TC formed during the season (Wang et al. 2007). It is noticed that the westward steering flow is stronger in ND than in JJASO, indicating a stronger signal of La Niña effect in the SCS in winter. Steering flow anomalies at the northern WNP and southwestern WNP till to IO are eastward, inhibiting landfalls at Korea and Japan.

To recapitulate, during the peak TC season of CP El Niño, the amount of eastward and westward moving TCs is comparable and the SCS is prevailed by weak eastward steering flow anomalies. During the peak TC season of EP El Niño, there are relatively more westward moving TCs (>76 %), while the SCS is also dominated by weak eastward steering flow anomalies. During autumn, there is a significant increase in the percentage of westward moving TCs in CP El Niño, EP El Niño and La Niña years comparing to that during summer. Westward moving TCs in EP El Niño and La Niña years are under the influence of westward steering flow anomalies. Therefore, in the peak TC season of CP El Niño and EP El Niño years, the steering flow anomalies in the SCS mostly favor eastward moving TCs. However, the eastward flow anomalies are too weak to exert enough impact on all TCs formed in the SCS. During the TC seasons (including JJASO and ND) of La Niña years, TCs in the SCS tends to move westward, matching well the westward steering flow anomalies.

6 Summary

This study investigates the mechanisms that modulate the directions of TCs in the SCS. It is found that majority of TCs during the peak TC season move westward, following the background TC steering flow, while the rest of TCs move eastward in association with anomalous TC steering flow induced by the ISO.

The composites of 20–100 day bandpass-filtered OLR and steering flow anomaly show that strong ISO activities and significantly large westerly steering flow occurs during eastward moving TC case. During westward TC cases, the area where most TCs generated in the SCS is mainly dominated by much weaker ISO activities and easterly steering flow. It is found that eastward moving TCs only appear during peak active phase of ISO with strong westerly anomalies that can overpower the background easterly. Westward moving TCs mainly occur during subactive phase of ISO, which induced weak westerly that can not overpower the background easterly.

There exists strong interannual variability in the moving direction of the TCs in the SCS. Whether this variability relates to ENSO effects is also discussed in this study. In the peak TC season of CP El Niño and EP El Niño years, the SCS was dominated by weak eastward steering flow anomalies. However, TCs did not predominantly move eastward, indicating weak impact of the large scale circulation in the two El Niño events. During the TC seasons (including JJASO and ND) of La Niña years, TCs in the SCS tends to move westward, possibly related to the westward steering flow anomalies.

Acknowledgments The authors thank Dr. Shang-ping Xie for valuable discussions. Suggestions by two anonymous reviewers significantly improved this paper. This work was supported by the National Basic Research Program of China (2011CB403504, 2012CB955603, 2010CB950302, 2013CB430301) and National Natural Science Foundation of China (41376025).

References

Ashok K, Behera SK, Rao SA, Weng H, Yamagata T (2007) El Niño Modoki and its possible teleconnection. J Geophys Res 112:C11007. doi:10.1029/2006JC003798

Camargo SJ, Sobel AH (2005) Western North Pacific tropical cyclone intensity and ENSO. J Clim 18:2996–3006

Camargo SJ, Sobel AH, Barnston AG, Emanuel KA (2007a) Tropical cyclone genesis potential index in climate models. Tellus 59A:428–443

Camargo SJ, Robertson AW, Gaffney SJ, Smyth P, Ghil M (2007b) Cluster analysis of typhoon tracks: part I: General Properties. J Clim 20:3635–3653

Camargo SJ, Robertson AW, Gaffney SJ, Smyth P, Ghil M (2007c) Cluster analysis of typhoon tracks: part II: large-scale circulation and ENSO. J Clim 20:654–3676

Camargo SJ, Wheeler MC, Sobel AH (2009) Diagnosis of the MJO modulation of tropical cyclogenesis using an empirical index. J Atmos Sci 66:3061–3074

Carr LE, Elsberry RL (1990) Observational evidence for predictions of tropical cyclone propagation relative to steering. J Atmos Sci 47:542–546

Chan JCL (1985) Tropical cyclone activity in the northwest Pacific in relation to the El Niño/Southern Oscillation phenomena. Mon Weather Rev 113:599–606

Chan JCL (1995) Prediction of annual tropical cyclone activity over the western North Pacific and the South China Sea. Int J Climatol 15:1011–1019

Chan JCL (2000) Tropical cyclone activity over the western North Pacific associated with El Nino and La Nina events. J Clim 13:2960–2972

Chan JCL, Gray WM (1982) Tropical Cyclone Movement and Surrounding Flow Relationships. Mon Weather Rev 110:1354–1374

Chan JCL, Xu M (2009) Inter-annual and inter-decadal variations of landfalling tropical cyclones in East Asia. Part I: time series analysis. Int J Climatol 29:1285–1293. doi:10.1002/joc.1782

Chan JCL, Liu K, Ching SE, Lai EST (2004) Asymmetric distribution of convection associated with tropical cyclones making landfall along the South China coast. Mon Weather Rev 132:2410–2420

Chen G (2011) How does shifting Pacific Ocean warming modulate on tropical cyclone frequency over the South China Sea? J Clim. doi:10.1175/2011JCLI4140

Chen T-C, Murakami M (1988) The 30–50-day variation of convective activity over the western Pacific Ocean with emphasis on the northwestern region. Mon Weather Rev 116:892–906

Chen G, Tam C-Y (2010) Different impacts of two kinds of Pacific Ocean warming on tropical cyclone frequency over the western North Pacific. Geophys Res Lett 37:L01803. doi:10.1029/2009GL041708

Chen TC, Wang SY, Yen MC, Clark AJ (2009) Impact of the intraseasonal variability of the western North Pacific largescale circulation on tropical cyclone tracks. Weather Forecast 24:646–666

Chia HH, Ropelewski CF (2002) The interannual variability in the genesis location of tropical cyclones in the Northwest Pacific. J Clim 15:2934–2944

Chu P-S, Kim J-H, Chen YR (2012) Have steering flows in the western North Pacific and South China Sea changed over the last 50 years? Geophys Res Lett 39:L10704

Dong K, Neumann C (1986) The relationship between tropical cyclone motion and environmental geostrophic flows. Mon Weather Rev 114:115–122

Du Y, Xie SP, Huang G, Hu K (2009) Role of air-sea interaction in the long persistence of El Nino-induced north Indian Ocean warming. J Clim 22:2023–2038

Du Y, Yang L, Xie SP (2011) Tropical Indian Ocean influence on Northwest Pacific tropical cyclones in summer following strong El Niño. J Clim 24(1):315–322. doi:10.1175/2010JCLI3890.1

Elsner JB, Liu K-B (2003) Examining the ENSO-typhoon hypothesis. Clim Res 25:43–54

Emanuel KA (1991) The theory of hurricanes. Ann Rev Fluid Mech 23:179–196

Franklin JL, Feuer SE, Kaplan J, Aberson SD (1996) Tropical cyclone motion and surrounding flow relationships: searching for beta gyres in omega dropwindsond datasets. Mon Weather Rev 124:64–84

Fudeyasu H, Iizuka S, Matsuura T (2006) Impact of ENSO on landfall characteristics of tropical cyclones over the western North Pacific during the summer monsoon season. Geophys Res Lett 33:L21815. doi:10.1029/2006GL027449

Gemmera M, Yin Y, Luo Y, Fischer T (2011) Tropical cyclones in China: county-based analysis of landfalls and economic losses in Fujian Province. Quat Int 244:69–177

Gill AE (1980) Some simple solutions for heat-induced tropical circulation. Q J R Meteorol Soc 106:447–462

Goh A, Chan JCL (2009) Interannual and interdecadal variations of tropical cyclone activity in the South China Sea. Int J Clim. doi:10.1002/joc.1943

Goh A, Chan JCL (2010) An improved statistical scheme for the prediction of tropical cyclones making landfall in South China. Weather Forecast 25:587–593

Gray WM (1979) Hurricanes: their formation, structure and likely role in the tropical circulation. In: Shaw DB (ed) Meteorology over the tropical oceans. R Meteorol Soc 155–218

Holland GJ (1983) Tropical cyclone motion: environmental interaction plus a beta effect. J Atmos Sci 40:328–342

Hong C–C, Li Y-H, Li T, Lee M-Y (2011) Impacts of central Pacific and eastern Pacific El Niños on tropical cyclone tracks over the western North Pacific. Geophys Res Lett 38:L16712

Huang P, Chou C, Huang RH (2011) Seasonal modulation of tropical intraseasonal oscillations on tropical cyclone geneses in the Western North Pacific. J Clim 24:6339–6352. doi:10.1175/2011JCLI4200.1

Kalnay E, Kanamitsu M, Kistler R et al (1996) The NCEP/NCAR 40-year reanalysis project. Bull Am Meteorol Soc 77:437–470

Kim J, Ho C, Kim H, Sui C, Park CK (2008) Systematic variation of summertime tropical cyclone activity in the western North Pacific in relation to the Madden–Julian oscillation. J Clim 21:1171–1191

Kim H-S, Kim J-H, Ho C-H, Chu P-S (2010) Pattern classification of typhoon tracks using fuzzy c-means clustering method. J Clim 24:488–508

Kim H-M, Webster PJ, Curry JA (2011) Modulation of North Pacific tropical cyclone activity by the three phases of ENSO. J Clim 24:1839–1849

Ko K, Hsu H (2009) ISO modulation on the submonthly wave pattern and recurving tropical cyclones in the tropical western north pacific. J Clim 22:582–599. doi:10.1175/2008JCLI2282.1

Kug J-S, Jin F–F, An S-I (2009) Two types of El Niño events: cold tongue El Niñ o and warm pool El Niño. J Clim 22:1499–1515

Lau KM, Chan PH (1985) Aspects of the 40–50-day oscillation during the northern winter as inferred from outgoing longwave radiation. Mon Weather Rev 113:1889–1909

Lee S-K, Wang C, Mapes BE (2009) A simple atmospheric model of the local and teleconnection responses to tropical heating anomalies. J Clim 22(2):227–284

Li CY, Zhou W (2013a) Modulation of Western North Pacific tropical cyclone activity by the ISO. Part I: genesis and intensity. J Clim 26:2904–2918. doi:10.1175/JCLI-D-12-00210.1

Li CY, Zhou W (2013b) Modulation of Western North Pacific tropical cyclone activity by the ISO. Part II: tracks and landfalls. J Clim 26:2919–2930. doi:10.1175/JCLI-D-12-00211.1

Li CY, Zhou W, Chan JCL, Huang P (2012) Asymmetric modulation of the Western North Pacific cyclogenesis by the Madden–Julian Oscillation under ENSO conditions. J Clim. doi:10.1175/JCLI-D-11-00337.1

Liang BQ (1991) Tropical atmospheric circulation system over the South China Sea. China Meteorology Press, Beijing, pp 100–224 (in Chinese)

Liebmann B, Smith C (1996) Description of a complete (interpolated) outgoing longwave radiation dataset. Bull Am Meteorol Soc 77:1275–1277

Liebmann B, Hendon HH, Glick JD (1994) The relationship between tropical cyclones of the western Pacific and Indian oceans and the Madden–Julian oscillation. J Meteorol Soc Jpn 72:401–411

Liu KS, Chan JCL (2003) Climatological characteristics and seasonal forecasting of tropical cyclones making landfall along the South China coast. Mon Weather Rev 131:1650–1662

Liu KS, Chan JCL (2008) Interdecadal variability of western North Pacific tropical cyclone tracks. J Clim 21:4464–4476

Liu KS, Chan JCL (2013) Inactive period of Western North Pacific tropical cyclone activity in 1998–2011. J Clim 26:2614–2630

Lyon B, Camargo SJ (2009) The seasonally-varying influence of ENSO on rainfall and tropical cyclone activity in the Philippines. Clim Dyn 32:125–141

Madden RA, Julian PR (1971) Detection of a 40–50 day oscillation in the zonal wind in the tropical Pacific. J Atmos Sci 28:702–708

Matsuno T (1966) Quasi-geostrophic motions in the equatorial area. J Meteorol Soc Jpn 44:25–43

Matthews AJ (2008) Primary and successive events in the Madden–Julian oscillation. Q J R Meteorol Soc 134:439–453. doi:10.1002/qj.224

Nakazawa T (1988) Tropical super clusters within intraseasonal variations over the western Pacific. J Meteorol Soc Jpn 64:17–34

Nakazawa T (1995) Intraseasonal oscillations during the TOGA-COARE IOP. J Meteorol Soc Jpn 73:305–319

Neumann CJ (1992) The Joint Typhoon Warning Center (JTWC92) model. SAIC final report, contract no. N00014-90-C-6042, 85 pp

Riley EM, Mapes BE, Tulich SN (2011) Clouds associated with the Madden–Julian oscillation: a new perspective from cloudsat. J Atmos Sci 68:3032–3051. doi:10.1175/JAS-D-11-030.1

Salby ML, Hendon HH (1994) Intraseasonal behavior of clouds, temperature, and motion in the tropics. J Atmos Sci 51:2207–2224

Saunders MA, Chandler RE, Merchant CJ, Roberts FP (2000) Atlantic hurricanes and NW Pacific typhoons: ENSO spatial impacts on occurrence and landfall. Geophys Res Lett 27:1147–1150

Sobel AH, Maloney ED (2000) Effect of ENSO and the MJO on the western North Pacific tropical cyclones. Geophys Res Lett 27:1739–1742

Sui C, Lau K (1992) Multiscale phenomena in the tropical atmosphere over the western Pacific. Mon Weather Rev 120:407–430

Tian H, Li C (2010) Further study of typhoon tracks and the low-frequency (30–60 days) wind-field pattern at 850 hPa. Atmos Ocean Sci Lett 3:319–324

Tian H, Li C, Yang H (2010) Modulation of typhoon tracks over the western North Pacific by the intraseasonal oscillation. Chin J Atmos Sci 4:559–579 (in chinese)

Wang B, Chan JCL (2002) How strong ENSO events affect tropical storm activity over the western North Pacific. J Clim 15:1643–1658

Wang Z, Fei L (1987) Manual for typhoon prediction. China Meteorology Press, Beijing, pp 260–287 (in Chinese)

Wang Y, Holland GJ (1996) The beta drift of baroclinic vortices. Part II: diabatic vortices. J Atmos Sci 53:3313–3332

Wang B, Li X (1992) The beta drift of three-dimensional vortices: a numerical study. Mon Weather Rev 120:579–593

Wang B, Rui H (1990) Synoptic climatology of transient tropical intraseasonal convection anomalies: 1975–1985. Meteorol Atmos Phys 44:43–61

Wang C, Wang X (2013) Classifying El Niño Modoki I and II by different impacts on rainfall in Southern China and typhoon tracks. J Clim 26:1322–1338. doi:10.1175/JCLI-D-12-00107.1

Wang B, Li X, Wu L (1997) Direction of hurricane beta drift in horizontally sheared flows. J Atmos Sci 54:462–1471

Wang L, Lau KH, Fung CH (2007) The relative vorticity of ocean surface winds from the QuikSCAT satellite and its effects on the geneses of tropical cyclones in the South China Sea. Tellus 59A:562–569

Wheeler MC, Hendon HH (2004) An all-season real-time multivariate MJO index: development of an index for monitoring and prediction. Mon Weather Rev 132:1917–1932

Wu CC, Emanuel KA (1995) Potential vorticity diagnostics of hurricane movement, Part I: a case study of Hurricane Bob (1991). Mon Weather Rev 123:69–92

Wu G, Lau NC (1992) A GCM simulation of the relationship between tropical storm formation and ENSO. Mon Wea Rev 120:958–977

Wu L, Wang B (2004) Assessing impacts of global warming on tropical cyclone tracks. J Clim 17:1686–1698

Wu M, Chang W, Leung W (2004) Impacts of El Niño-Southern Oscillation events on tropical cyclone landfalling activity in the western North Pacific. J Clim 17:1419–1428

Wu L, Wen Z, Huang R, Wu R (2012) Possible linkage between the monsoon trough variability and the tropical cyclone activity over the Western North Pacific. Mon Weather Rev 140:140–150. doi:10.1175/MWR-D-11-00078.1

Xie SP, Xie Q, Wang D, Liu WT (2003) Summer upwelling in the South China Sea and its role in regional climate variations. J Geophys Res 108:3261. doi:10.1029/2003JC001867

Xie SP, Hu KM, Hafner J, Tokinaga H, Du Y, Huang G, Sampe T (2009) Indian Ocean capacitor effect on Indo-Western Pacific climate during the summer following El Nino. J Clim 22:730–747

Yang L, Du Y, Xie SP, Wang D (2012) An inter-decadal change of tropical cyclone activity in the South China Sea in early 1990s. Chin J Oceanol Limnol 30(6):138–144. doi:10.1007/s00343-012-1258-9

Yonekura E, Hall TM (2011) A Statistical model of tropical cyclone tracks in the western North Pacific with ENSO-dependent cyclogenesis. J Appl Meteorol Climatol 50:1725–1739

Zhan R, Wang Y, Lei X (2011) Contributions of ENSO and East Indian Ocean SSTA to the interannual variability of Northwest Pacific tropical cyclone frequency. J Clim 24:509–521. doi:10.1175/2010JCLI3808.1

Zhang W, Graf H-F, Yee Leung, Michael Herzog (2012) Different El Niño types and tropical cyclone landfall in East Asia. J Clim 24:6510–6523. doi:10.1175/JCLI-D-11-00488.1

Zhang W, Leung Y, Chan JCL (2013) The analysis of tropical cyclone tracks in the western North Pacific through data mining. Part I: tropical cyclone recurvature. J Appl Meteorol Climatol 52:1394–1416